

A comparative model for anisothermal and isothermal crystallization of poly(ethylene terephthalate)

A. Douillard*[‡], Ph. Dumazet*[‡], B. Chabert* and J. Guillet[†]

* *Laboratoire d'Études des Matériaux Plastiques et des Biomatériaux, URA CNRS No. 507, Université 'Claude Bernard' Lyon I, 43 Boulevard du 11 Novembre 1918, 69622 Villeurbanne Cedex, France*

[†] *Laboratoire de Rhéologie des Matières Plastiques, Université des Sciences, 23 Rue du Dr Paul Michelon, 42023 Saint Etienne Cedex 02, France*

(Received 16 April 1991; revised 4 March 1992)

A new method for analysing and modelling anisothermal crystallization from a polymer melt is proposed in a way allowing comparison with isothermal conditions, and supposing that no variation of the process occurs in the whole temperature range. The model is based on a modified Avrami equation: $1 - U = \exp\{-K(T)[(T_\alpha - T)/\alpha]^n\}$, where the starting point T_α , highly dependent on the cooling rate α , appears to be of major importance. Some methods for its determination are derived. Application to crystallization kinetics of poly(ethylene terephthalate) by differential scanning calorimetry is discussed and a comparison of both methods shows good accuracy. Moreover, anisothermal studies allow a more extended temperature range for $K(T)$ determination and seem more closely connected with the current value of apparent n , interpreted in terms of a dual mechanism. Finally an equation describing $K(T)$ variations is proposed and allows one to describe quantitatively any anisothermal process, particularly at the beginning, which is suitable for setting conditions.

(Keywords: poly(ethylene terephthalate); crystallization; isothermal; anisothermal; kinetics; model)

INTRODUCTION AND THEORY

The crystallization kinetics of poly(ethylene terephthalate) (PET) have largely been studied under isothermal conditions and also under anisothermal conditions at constant cooling rates. The most common experimental method is thermal analysis (d.t.a. or d.s.c.), from which data are respectively interpreted in terms of Avrami–Evans^{1,2} or Ozawa³ equations. But, generally, both methods are not easy to connect and some discrepancies occur between comparable values.

Our purpose is to extend to PET a method recently developed by one of us⁴ for poly(butylene terephthalate), which allows one to make comparative determinations of Avrami exponents and Avrami constants from both isothermal and anisothermal experiments.

In addition, anisothermal measurements for high cooling rates can be performed over a more extended temperature range, whereas the accessible range for isothermal conditions is limited to low undercooling temperatures.

Moreover, in order to enquire into the optimum conditions for an industrial process, it is necessary to have a procedure for a quantitative description of non-isothermal crystallization processes at practicable cooling rates^{5–9}.

Isothermal kinetics are based on the Avrami equation:

$$1 - U = \exp[-K(T)t^n] \quad (1)$$

and anisothermal kinetics are based on the derived Ozawa equation:

$$1 - U = \exp[-\chi(T)/\alpha^n] \quad (2)$$

where U is the volume fraction of transformed polymer (spherulites for PET), t is time, $K(T)$ is a temperature-dependent coefficient, $\chi(T)$ is the cooling function, α is the cooling rate ($\alpha > 0$), and n and n' are characteristic exponents. Often other extrapolations of isothermal to anisothermal conditions lead to relatively complicated equations^{10,11} even if the temperature gradient is not taken into account. It is important to notice that, even if $K(T)$ is dependent on the nucleation conditions, the crystallization rate is described by equation (1) only after a delay time necessary to obtain supercritical nuclei. In other words, the time parameter must be related to the experimental effective start of growth.

If every anisothermal process of crystallization is assumed to be a series of infinitely narrow isothermal processes governed by equation (1) with a quite constant exponent n over the whole temperature range, the time parameter can then be substituted for the temperature according to:

$$T_\alpha - T = \alpha(t - t_\alpha) \quad (3)$$

where $\alpha > 0$ is the constant cooling rate, and T_α and t_α respectively are the starting temperature and the starting time. Then:

$$1 - U = \exp\{-K(T)[(T_\alpha - T)/\alpha]^n\} \quad (4)$$

[‡] To whom correspondence should be addressed

0032-3861/93/081702-07

© 1993 Butterworth-Heinemann Ltd.

As equations (2) and (4), both derived from equation (1), need the same constancy of mechanism, they represent the same temperature dependence only if for any α value:

$$K(T)(T_\alpha - T)^n = \chi(T)$$

It is experimentally evident that T_α decreases with increasing α values and thus $\chi(T)$ determinations change all the more so since the temperature is closer to T_α . This point can be clearly observed for many polymers besides PET (poly(butylene terephthalate) (PBT), polyamide (PA), poly(phenylene sulfide) (PPS), etc.), particularly from d.s.c. endotherms even after temperature correction for the scanning rate dependence. Other anisothermal experiments involving crystallization, such as rheological parameters¹², also present this phenomenon. It can also be interpreted qualitatively from the nucleation delay, dependent on the temperature.

The purpose of this paper is to show that, for PET, anisothermal data interpreted in terms of equation (4) can give an interesting extension for n and $K(T)$, compared to the values determined by the isothermal method.

The crystallization mechanism from the melt of this polymer seems to be the same over the whole temperature range with n close to 3 according to athermal (heterogeneous) nucleation.

The proposed method consists of plotting the double logarithmic relation derived from equation (4) versus $\ln[(T_\alpha - T)/\alpha]$ for some different cooling rates according to:

$$\ln[-\ln(1-U)] = \ln[K(T)] + n \ln[(T_\alpha - T)/\alpha] \quad (5)$$

Isothermal points of the plot give a set of straight lines from which, as for the isothermal method, n and $K(T)$ can be calculated respectively from the slope and intercept, for a continuum of temperature values.

The first major problem for the accuracy of each α value plot is the previous determination of T_α , the actual starting point. For d.s.c. plots, visual evaluations give experimental precisions of about 0.4°C.

According to this case and also other methods, the derivative dU/dt can be calculated from experimental data; some equations, using these values, can be derived from equation (5). The derivative with respect to time is:

$$\frac{-dU/dt}{(1-U)\ln(1-U)} = \frac{n\alpha}{T_\alpha - T} \left[1 - \frac{\partial K}{K n \partial T} (T_\alpha - T) \right] \quad (6)$$

and the derivative with respect to $\ln[(T_\alpha - T)/\alpha]$ is:

$$p = \frac{d \ln[-\ln(1-U)]}{d \ln[(T_\alpha - T)/\alpha]} = n - \frac{\partial K}{K \partial T} (T_\alpha - T) \quad (7)$$

Further development needs hypotheses on the values and variations of the correcting term $(T_\alpha - T) \partial K / K \partial T$ in the vicinity of T_α , n being constant. This point is discussed in the appendix from experimental results for PET and also, but not exhaustively, for related polymers. It is shown that this function exhibits a quite constant value in a 10°C temperature range:

$$-\frac{\partial K}{K \partial T} (T_\alpha - T) = p - n = \text{constant}$$

Thus equation (7) leads to a power-law approximation for $K(T)$ given by (A1):

$$K(T) = A(T_\alpha - T)^{p-n}$$

In these conditions the inverse of equation (6) is quite linear:

$$\frac{(1-U)\ln(1-U)}{dU/dt} = -\frac{T_\alpha - T}{p\alpha} \quad (8)$$

Then T_α can be determined from the intercept of the plot at $U=0$. The parameter p can also be calculated from the value of the slope $1/p\alpha$ in the same limiting conditions. Equation (4) can be approximated by its first-order expansion. Combination with equation (A1) gives:

$$U = \frac{A}{\alpha^n} (T_\alpha - T)^p$$

from which a second linear relation is obtained for T_α extrapolation at $U=0$:

$$U^{1/p} = B(T_\alpha - T) \quad (9)$$

Similar equations can also be derived from isothermal data for the same kind of determinations of the starting time t_0 . The first linear equation from the derivative of the double logarithmic function is exactly:

$$-\frac{(1-U)\ln(1-U)}{dU/dt} = \frac{t-t_0}{n} \quad (10)$$

from which the Avrami exponent in the vicinity of zero is also obtained by plotting the second and approximate equation:

$$U^{1/n} = B(t-t_0) \quad (11)$$

EXPERIMENTAL

We used two classical (linear) PET samples supplied by Rhône-Poulenc; one peculiar characteristic is defined according to g.p.c. results made on PET calibrated silica-gel columns.

Moreover, intrinsic viscosity measurements (IV), with the help of a SEPTEM automatic viscosimeter, are performed in 50/50 (vol) phenol/tetrachloroethane solutions, according to the Mark-Houwink-Sakurada equation:

$$[\eta] = 4.68 \times 10^{-4} (\bar{M}_w)^{0.68} \quad (12)$$

Table 1 summarizes the chemical and molecular characterizations. For crystallization kinetics a Perkin-Elmer DSC4 calorimeter is used. The computing unit allows one to determine all the previously mentioned functions.

Table 1 Molecular characteristics of resins^a

	PET A	PET B
Polymerization process	Melt-phase transesterification of DMT/EG	Melt-phase esterification of TPA/EG
Catalyst system	Sb ₂ O ₃ + AcMn	Sb ₂ O ₃
\bar{M}_n g.p.c. (g mol ⁻¹)	19 500	17 000
\bar{M}_w g.p.c. (g mol ⁻¹)	39 000	43 000
$\bar{M}_w IV$ (g mol ⁻¹)	36 000	45 000
$I_p = \bar{M}_w / \bar{M}_n$	2	2.5
DEG (mol%)	0.75	1.05
Stabilizer additives	None	Irganox

^a Abbreviations: DMT/EG, dimethyl terephthalate/ethylene glycol; TPA/EG, terephthalic acid/ethylene glycol; IV , intrinsic viscosity; DEG, diethylene glycol

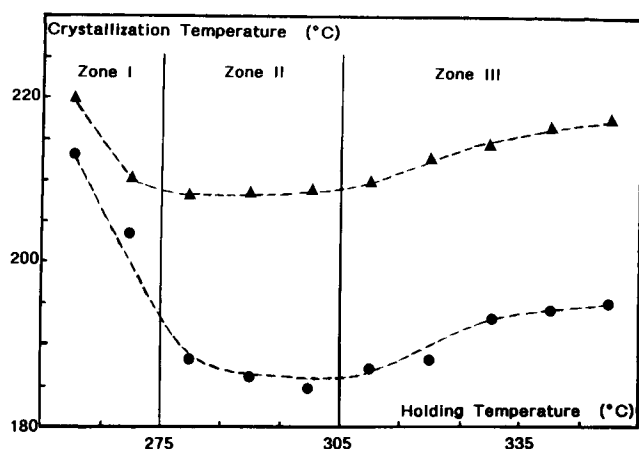


Figure 1 Maximum of exothermic crystallization peaks at $10^{\circ}\text{C min}^{-1}$ versus holding temperature for 6 min: (\blacktriangle) for sample A; (\bullet) for sample B

Calibration is made with indium ($T_m = 155.6^{\circ}\text{C}$, $\Delta H = 6.8 \text{ cal g}^{-1}$) at $10^{\circ}\text{C min}^{-1}$. Temperature scale translation was established for all heating or cooling rates.

Polymer samples of about 15 mg are placed in crimped aluminium pans with holes for nitrogen circulation to prevent oxidative degradation. A new sample is used for each measurement, as it is found that poor thermal stability allows no more than two identical runs.

Samples are heated at $60^{\circ}\text{C min}^{-1}$ to 285°C , held there for 6 min to remove the thermal history and then crystallized from the melt as follows:

(i) for isothermal measurements, by cooling at $200^{\circ}\text{C min}^{-1}$ to the appropriate values 220, 225, 230 and 235°C for sample A and 200, 210, 220 and 225°C for sample B;

(ii) for anisothermal measurements, at scanning rates of 1, 2, 4, 8, 10, 15 and $20^{\circ}\text{C min}^{-1}$ for both sample types.

RESULTS AND DISCUSSION

The first preliminary problem for the processing of PET at high temperatures concerns the drying conditions in order to avoid any molecular evolution of this polycondensate. The 0.3% moisture absorbed in open air is removed within 5 h at 150°C under vacuum. Otherwise, if the polymer is left in open air and melted at 285°C for 6 min, the molecular weight measured by IV collapses to about one-half of its previous value and correspondingly the crystallization kinetics are widely modified. These results are in good accordance with the literature, where Jabarin^{13,14} noticed that moisture has a great influence on crystallization by reducing the molecular weight and thus by increasing the nucleation rate. It is worth noting that a further rheological study has fully confirmed these results¹⁵.

Finally the polymer is stored in an air oven at $100\text{--}105^{\circ}\text{C}$, and under these conditions the crystallization kinetics remain identical over many months.

The second point concerns the disappearance of the thermal history after melting the polymer. To work out these conditions, samples are kept for 6 min at various temperatures and then crystallized anisothermally at $10^{\circ}\text{C min}^{-1}$. Figure 1 shows the experimental plot of the maximum value of the exothermic peak, considered as representative of the crystallization interval.

(I) For $T < 275^{\circ}\text{C}$ the decreasing values can be

interpreted as a progressive disappearance of remaining supercritical crystallites.

(II) Between 275 and 305°C the kinetics occur in the same conditions.

(III) Over 305°C the maximum values increase. This may be due to a molecular change resulting from chain scission and crosslinking.

Practically, a holding time of 6 min at 285°C seems to be suitable for removing completely the thermal history without appreciable molecular change, as shown by the constancy of IV. These conditions are close to those in the literature: Hartley¹⁶ and Jackson¹⁷ ($294^{\circ}\text{C}/10 \text{ min}$); Jabarin¹⁸ ($294^{\circ}\text{C}/15 \text{ min}$); Fielding Russel¹⁹ ($277^{\circ}\text{C}/15 \text{ min}$); and Van Antwerpen²⁰ ($285^{\circ}\text{C}/3 \text{ min}$).

A complex mechanism of crystallization for PET—among other polymers—has been pointed out and discussed by Chang Zhou²¹ and Sweet²² on the grounds of three endotherms observed by subsequent meltings after isothermal crystallizations. This behaviour is also observed for the PET samples studied in this paper. Evidence is shown in Figure 2 for PET A, entirely crystallized at 200°C . The three peaks are labelled I, II and III respectively corresponding to increasing temperatures. Further experimental study ascertains that peak I occurs about 10°C above the crystallization temperature only after a delay of 3 min. It characterizes this anomalous behaviour and remains at the same discrepancy of about 10°C for higher isothermal temperatures but it is less and less important. A tedious kinetic analysis of these small crystallites consisting of melting them at $10^{\circ}\text{C min}^{-1}$ for various crystallization times at 200°C is performed for sample A. It shows an Avrami behaviour with n close to 1.5. This method leads to poor accuracy. According to this weak n value, this process could be interpreted by secondary nucleated growth on already existing crystals—related to peak II—but hindered by a more entangled melted phase. Another explanation for this peak could be the crystal growth of cyclic oligomer in accordance with its maximum value around 190°C ²³. But the evolution of its melting temperature for a long time (more than 5 h at 200°C) is in disagreement with this assumption because peak I disappears and the global enthalpy measured on peaks II and III increases by a few per cent. Concerning peak III, it is now well known from the literature that it occurs from melting and recrystallization of peak II.

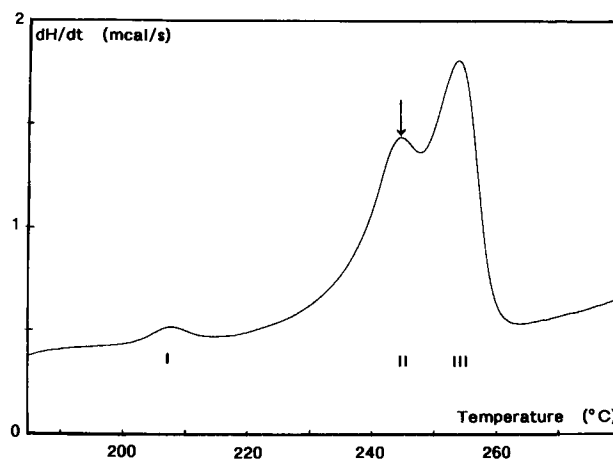


Figure 2 Three melting peak endotherms for PET B isothermally crystallized at 200°C for 20 min; scanning rate $10^{\circ}\text{C min}^{-1}$; peak II shows the melting temperature T_m

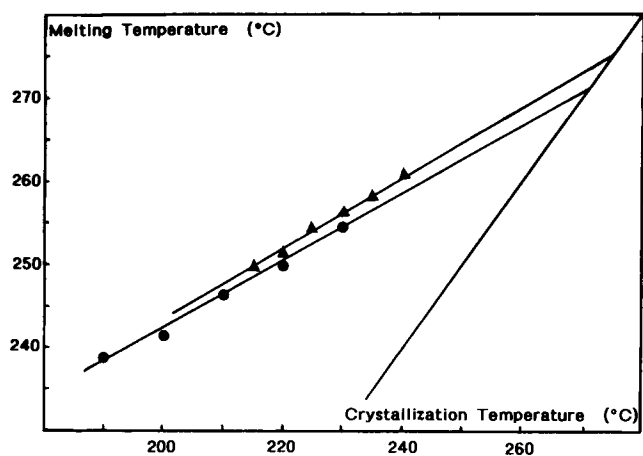


Figure 3 Hoffman's plot of melting temperature T_m of peak II versus isothermal crystallization temperature: (\blacktriangle) for sample A; (\bullet) for sample B

Table 2 Comparison between isothermal and anisothermal results (K in min^{-n})

Sample	Isothermal			Anisothermal		
	T ($^{\circ}\text{C}$)	n	$\ln(K)$	ΔH_{∞} (cal g^{-1})	n	$\ln(K)$
A	220	2.63	-2.49	10.36	2.72	-1.55
	225	2.83	-3.75	11.09	2.88	-3.90
	230	2.79	-5.15	10.23	2.89	-5.30
	235	2.81	-7.50	8.73	2.89	-7.45
B	200	2.66	-3.05	9.56	2.54	-3.15
	210	2.71	-4.70	8.66	2.54	-5.03
	220	2.79	-6.87	8.62	2.66	-7.08
	225	2.78	-8.10	8.76	2.57	-8.20

This lower-temperature peak I is also observed for anisothermal crystallizations. Whatever the origin of this phenomenon, not yet clearly understood, the isothermal double logarithmic plots remain straight lines for $U < 0.7$ and it is not possible to derive both kinetics from them without any modelling: the effect which is expected is probably just a slight variation for n . It can certainly not be confused with the end of the kinetics (for $U > 0.7$) for which n falls down also close to 1 and characterizes the end of the spherulitically hindered growth.

In addition, maximum melting temperatures T_m can be set according to Hoffman²⁴. Melting temperatures of peak II are plotted in Figure 3: $T_m = 275^{\circ}\text{C}$ for sample A and $T_m = 271^{\circ}\text{C}$ for sample B. These values are in accordance with the lower limit of temperature to remove the thermal history. This is what many authors have noticed: Wunderlich²⁵ and Mehta²⁶ have found 280°C ; Smith²⁷ and Fielding Russel¹⁹ 267°C and 269°C ; Colomer Vilanova²⁸ 266°C to 273°C depending on the molecular weight; and Phillips²⁹ 278°C .

From isothermal kinetics with the use of t_0 , according to equations (10) and (11), double logarithmic plots give the values of n and $K(T)$ summarized in Table 2.

As for anisothermal kinetics, Figure 4 shows d.s.c. curves from sample B obtained after subtracting the baselines. As explained in the appendix, experimental dU/dt and U values can be calculated by plotting equation (8) and afterwards equation (9) from the p values

obtained. Figure 5 shows plots for some scanning rates of PET B, and Table 3 summarizes the extrapolated T_x values. On this plot the first points are significantly curved away from the straight line. This is due to the high experimental error in dH/dt close to the baseline and worsened by the integer number structure of the data. Thus they are not taken into account for the least-squares determinations.

An empirical linear relationship between T_x and $\sqrt{\alpha}$ is established for both sample types as seen in Figure 6. On this plot, sample A seems to give less regular variations for T_x . But it is a general observation for d.s.c. curves that, for the same experimental conditions (cooling rates, weights, etc.), a stochastic temperature shift as high as 2°C for higher cooling rates can be observed. This fact is certainly due to the variation of the temperature gradient within the sample, which is highly dependent on the thermal conductance between the oven, the pan and the polymer.

Concerning the conditions to obtain reasonable crystallinity values after complete crystallization, the upper limit for α is $20^{\circ}\text{C min}^{-1}$ for sample A and $15^{\circ}\text{C min}^{-1}$ for sample B.

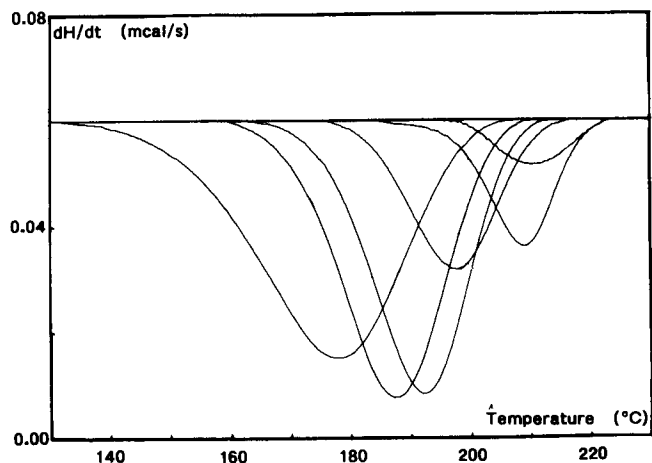


Figure 4 Plot of anisothermal crystallization exotherms for PET B at various cooling rates: 15, 10, 8, 4, 2 and $1^{\circ}\text{C min}^{-1}$ according to increasing temperatures

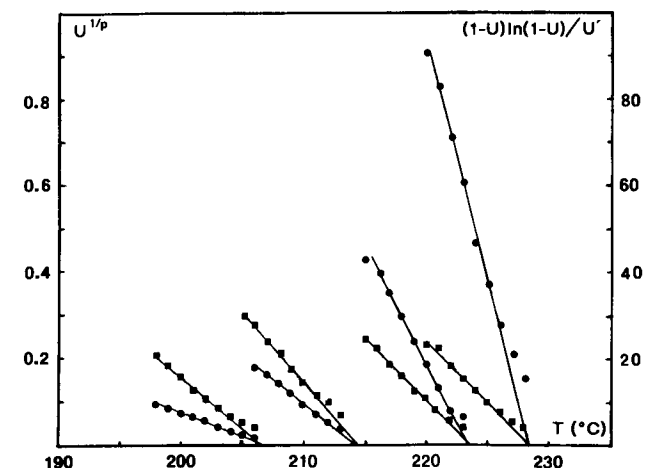


Figure 5 Determination of starting temperature T_x for sample B: (\blacksquare) from equation (7) and (\bullet) from equation (8) for cooling rates respectively 20, 10, 4 and $2^{\circ}\text{C min}^{-1}$ according to increasing temperatures

Table 3 Results from anisothermal scans

Sample	α ($^{\circ}\text{C min}^{-1}$)	1	2	4	5	8	10	15	20
A	T_x ($^{\circ}\text{C}$)	238.4	235.2	233.6	231.2	227.6	224.6	219.7	214.8
	p	3.30	8.35	3.25	3.30	3.45	3.30	3.40	3.15
	ΔH_{∞} (cal g^{-1})	10.9	10.01	10.82	10.75	10.89	10.32	10.57	10.44
B	T_x ($^{\circ}\text{C}$)	231.6	228.8	223.5	—	217.5	214.3	208.4	206.5
	p	3.30	3.40	3.40	—	3.50	3.45	3.35	3.30
	ΔH_{∞} (cal g^{-1})	9.65	9.71	9.10	—	8.92	9.15	7.49	6.25

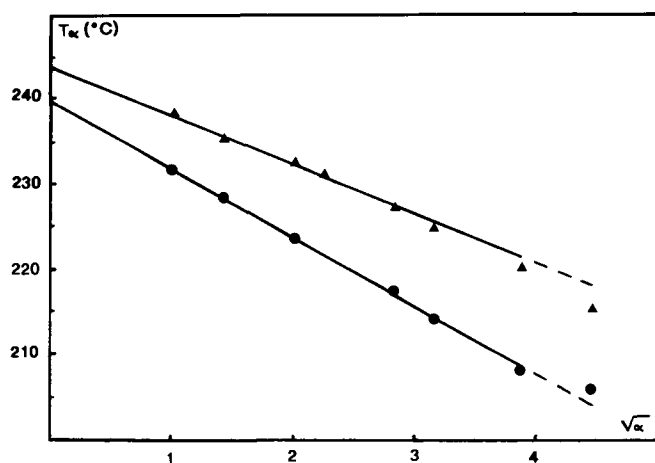


Figure 6 Plot of starting temperature versus $\sqrt{\alpha}$ (α in $^{\circ}\text{C min}^{-1}$): (\blacktriangle) for sample A; (\bullet) for sample B

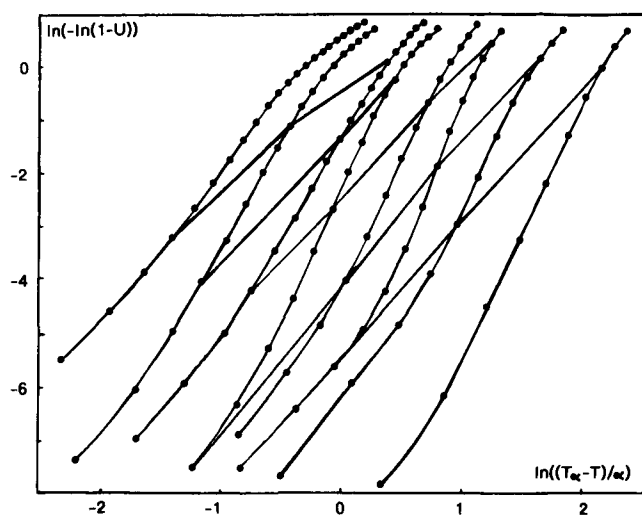


Figure 7 Anisothermal double logarithmic plot for sample A at respectively 20, 15, 10, 8, 5, 4, 2 and $1^{\circ}\text{C min}^{-1}$ according to increasing abscissae. Isothermal lines are drawn at respectively 230, 225, 220, 215 and 210°C according to increasing ordinates

Figures 7 and 8 show the complete double logarithmic plots, from which each curve is approximately linear. From equation (9) the variation of slope is mainly due to the last term including the derivative of $\ln(K)$. At the limits of the temperature interval for the highest values or for values close to the maximum of the

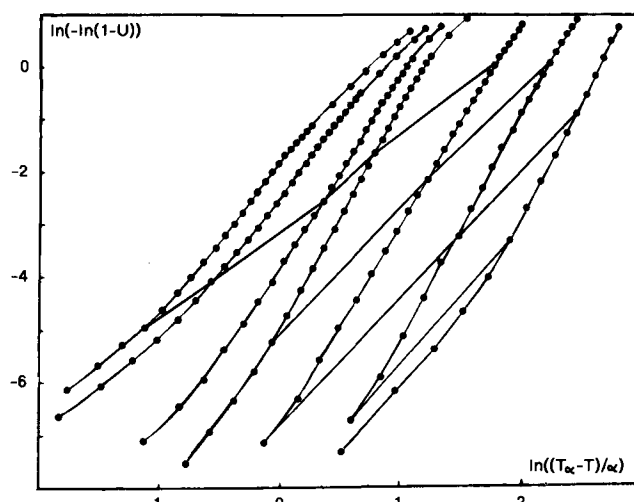


Figure 8 Same plot as Figure 7 but for sample B at 20, 15, 10, 8, 4, 2 and $1^{\circ}\text{C min}^{-1}$ with isothermal lines at 225, 220, 210 and 200°C

crystallization peak, slopes are close to 3; and for the middle part, they are higher than 4. The interesting parts of the plots (for $U < 0.7$) allow one to determine $K(T)$ in the intervals 200 to 230°C for sample A and 180 to 225°C for sample B with complete isothermal lines. Extension can be made under and over these values by using parallel lines in continuity with the previous ones. Table 2 allows comparisons between isothermal and anisothermal determinations. Although the agreement is less accurate for sample B, it is quite good and a plot of $\ln(K)$ is given in Figure 9 for both samples.

In the experimental ranges of crystallization temperatures, $\ln(K)$ can be well represented by the following equation, derived from the literature²⁵:

$$\ln(K) = A - \frac{B}{T - T_0} - \frac{CT_m}{T^2(T_m - T)} \quad (13)$$

where A , B and C are constants, A depending on molecular weight; T_0 is the limiting lower temperature for which no further transport occurs near the growing crystal; and T_m is the maximum melting temperature. As shown in Figure 9 the following values fit equation (13):

$$\begin{aligned} A_A &= 25.95 \text{ for sample A} & A_B &= 22.8 \text{ for sample B} \\ B &= 1195 \\ C &= 525\,000 \\ T_0 &= 329 \text{ K} \end{aligned}$$

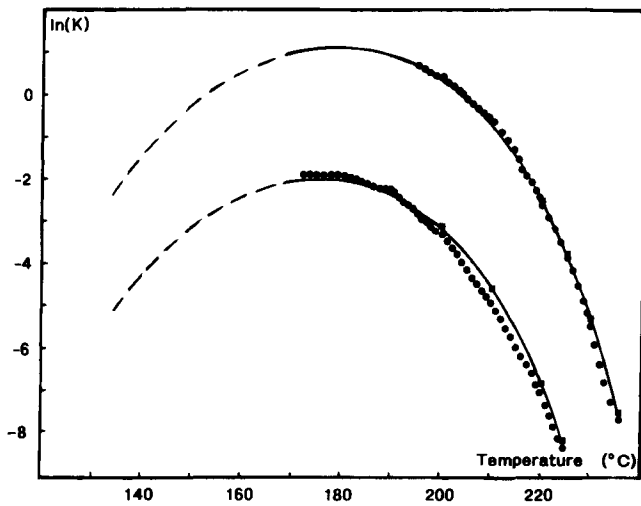


Figure 9 Plot of $\ln(K)$ (K in min^{-n}) versus temperature: (■) from isothermal results; (●) from anisothermal. The upper plot is for sample A, the lower for sample B

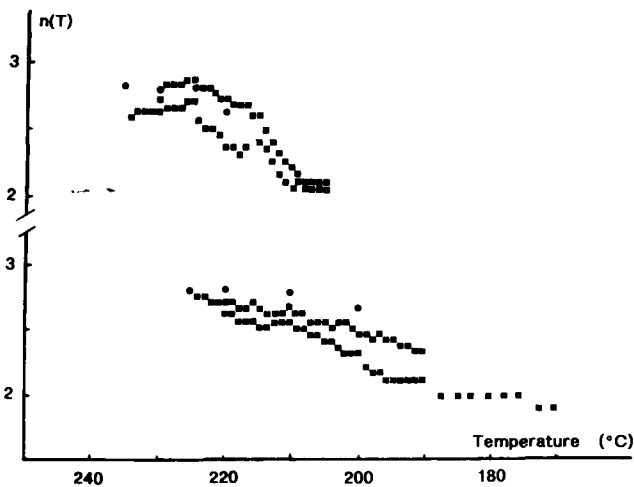


Figure 10 Plot of Avrami exponents: (■) from anisothermal results; (●) from isothermal. The upper plot is for sample A, the lower for sample B

with T_m as previously determined:

$$T_{mA} = 549 \text{ K} \quad T_{mB} = 545 \text{ K}$$

It is worth noting that the maxima for $\ln(K)$ occur respectively at $T_{\max} = 453 \text{ K}$ (180°C) and $T_{\max} = 449 \text{ K}$ (176°C) for sample A and sample B, which are close to the value $0.82T_m$.

As for the exponent n , the tendency to increase with temperature seems confirmed from isothermal and anisothermal results (Table 2). On the other hand, for a given cooling rate, n decreases from its starting value with increasing supercooling ΔT , as shown in Figure 10. This point is in good agreement with the previously discussed anomalous crystallization occurring during main growth, all the more so since the temperature is lower and modifies the kinetics.

A descriptive model for anisothermal crystallization of PET can be derived from equation (13). Figure 11 shows experimental and calculated values for sample B at $\alpha = 4$ and 8°C min^{-1} for which $n = 2.7$ for $T > 210^\circ\text{C}$ and linearly varying between 2.7 and 2.2 for $180^\circ\text{C} < T < 210^\circ\text{C}$. Agreement is quite good for the interesting part at $U < 0.7$.

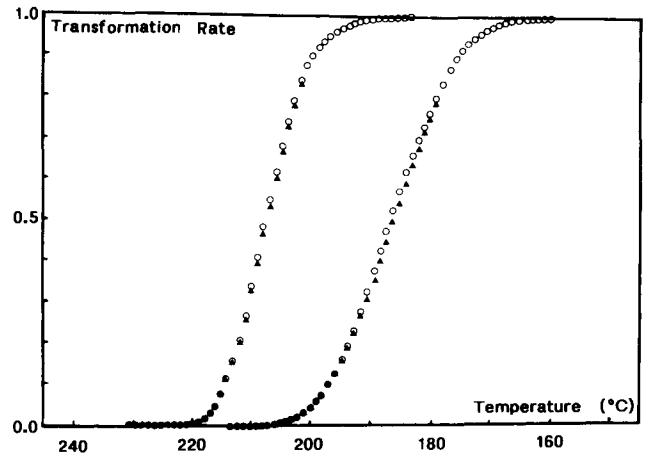


Figure 11 Transformation rates for sample B crystallized at 4°C min^{-1} (left plot) and $10^\circ\text{C min}^{-1}$ (right plot): (○) experimental and (▲) calculated

CONCLUSION

Although it is tedious, the characterization of PET crystallization from anisothermal data seems very attractive. The agreement with the derived Avrami equation is quite good and moreover the proposed method allows one to have a more extended range at lower temperature in order to determine $K(T)$. This makes possible a descriptive model for anisothermal crystallization kinetics from the melt under various conditions. Finally, the crystallization of this polymer is not simple and needs further studies to describe it in a more scientific way.

ACKNOWLEDGEMENTS

This work was supported by PSA (Peugeot Société Anonyme) to which one of us expresses his thanks for the provision of a studentship.

REFERENCES

- Avrami, M. J. *Chem. Phys.* 1939, **7**, 1103; 1940, **8**, 212
- Evans, M. *Trans. Faraday Soc.* 1945, **41**, 365
- Ozawa, T. *Polymer* 1970, **12**, 150
- Douillard, A. *C.R. Acad. Sci., Paris (Ser. II)* 1990, **311**, 1405
- Malkin, A. Ya., Beghishev, V. P. and Keapin, I. A. *Polymer* 1983, **24**, 81
- Malkin, A. Ya., Beghishev, V. P., Keapin, I. A. and Andrianova, Z. S. *Polym. Eng. Sci.* 1984, **24**, 1396
- Malkin, A. Ya., Beghishev, V. P., Keapin, I. A. and Andrianova, Z. S. *Polym. Eng. Sci.* 1984, **24**, 1402
- Lee, K. H. and Kim, S. C. *Polym. Eng. Sci.* 1988, **28**, 13
- Addonizio, M. L., Martuscelli, E. and Silvestre, C. *Polymer* 1987, **28**, 183
- Rein, D. M., Beder, L. M., Baranov, V. G. and Chegolya, A. S. *Acta Polym.* 1981, **32**, 1
- Choe, C. R. and Lee, K. H. *Polym. Eng. Sci.* 1989, **29**, 12, 801
- Moore, L. D. ACS Meeting, Cleveland, 1960, Vol. 1
- Jabarin, S. A. *J. Appl. Polym. Sci.* 1987, **34**, 103
- Jabarin, S. A. *Polym. Eng. Sci.* 1984, **24**, 13, 1056
- Dumazet, Ph., Chabert, B., Douillard, A., Guillet, J., Gérard, A. and André, G. III EPF Congress, Sorrento, Italy, 1990, p. 130
- Hartley, F. D., Lord, F. W. and Morgan, L. B. *Philos. Trans. R. Soc. London (A)* 1954, **247**, 23
- Jackson, J. B. and Longman, G. W. *Polymer* 1969, **10**, 873
- Jabarin, S. A. *J. Appl. Polym. Sci.* 1987, **34**, 85
- Fielding Russel, G. S. and Pillar, P. S. *Makromol. Chem.* 1970, **135**, 263
- Van Antwerpen, F., PhD Thesis, University of Nijmegen, 1971

- 21 Zhou, C. and Clough, S. B. *Polym. Eng. Sci.* 1988, **28**, 2, 65
 22 Sweet, G. E. and Bell, J. P. *J. Polym. Sci.* 1972, **10**, 1273
 23 Linz, C. C., *Plastics Meeting Challenges of the Future, SPE Annu. Tech. Conf.* 1982, **40**, 901
 24 Hoffman, J. D. and Weeks, J. J. *J. Res. Nat. Bur. Std* 1962, **66A**, 13
 25 Wunderlich, B. *Macromol. Phys.* 1980, **3**, 68
 26 Mehta, A., Gaur, U. and Wunderlich, B. *J. Polym. Sci., Polym. Phys. Edn* 1978, **16**, 289
 27 Smith, C. W. and Dole, M. J. *Polym. Sci.* 1956, **10**, 37
 28 Colomer Vilanova, P., Montserrat, S. and Martin-Guzman, G. *Polymer* 1985, **26**, 423
 29 Phillips, P. J. and Tseng, H. T. *Macromolecules* 1989, **22**, 1649

$$p = n - \frac{\partial K}{K \partial T} (T_x - T)$$

is quite constant in a temperature range of 10°C at the most and stays at values close to n :

$$3 < p < 3.5$$

As $\partial K/K \partial T < 0$ and assuming $n = 2.5$:

$$0.5 < -\partial K/K \partial T < 1.5$$

Integration of equation (7) then gives:

$$K(T) = A(T_x - T)^{p-n} \quad (\text{A1})$$

For example, for PET B at $\alpha = 15^\circ\text{C min}^{-1}$, T_x is close to 220°C and the first fitting gives:

$$K(T) = 6.41 \times 10^{-4} (220 - T)^{1.04}$$

with a coefficient of correlation of 0.981. In the same 10°C range, final results give:

$$K(T) = 6.41 \times 10^{-4} (219.7 - T)^{0.96}$$

and the coefficient of correlation is then 0.979.

This empirical approximation seems accurate and is very convenient. As for PET, attempts have been made for analogous polymers concerning their crystallization behaviour, such as PBT and also PPS, and have confirmed this result. Nevertheless, it would be desirable to extend this to a wider range of polymers.

APPENDIX

The problem is to have approximations of the term $(T_x - T) \partial K/K \partial T$ in the vicinity of T_x in equations (6) and (7). In order to avoid any vicious circle, it is necessary to derive them intrinsically from experimental data. For each peak, dH/dt values can be obtained by the discrepancy from an extended line tangentially connected at its ends to the baseline and from which T_x can be evaluated. The volumic rates U can then be obtained by integration and with suitable corrections can be used for plotting equation (5) in a first iteration. In the case of PET A and B, for any scanning rate, the measured slope p according to equation (7):